Model of a Twin-Screw Extruder Operating with a Cryocooler for the Solidification of Deuterium

J.W. Leachman, J.M. Pfotenhauer, G.F. Nellis

University of Wisconsin-Madison
Madison, WI 53706

ABSTRACT

This paper discusses the modeling of a twin-screw extruder, cooled by a Gifford McMahon cryocooler, for the generation of solid deuterium pellets. A numerical model of the extruder is developed, in order to simulate the solidification of deuterium over a range of operating conditions and extruder design parameters. The numerical model integrates a set of governing differential equations in the flow direction and includes variations in the thermodynamic and transport properties of the deuterium and extruder material as well as the effect of viscous energy dissipation and the latent heat of solidification. The model is used to evaluate the sensitivity of the extruder performance to the various parameters and processes in order to identify the critical areas for future experimental efforts.

INTRODUCTION

Deuterium extrusion research is important for fusion energy. The fuels for fusion energy are the heavy isotopes of hydrogen. The hydrogen isotopes protium, deuterium, and tritium combine in an environment like earth to form the isotopic and non-isotopic molecules shown in Figure 1. Although the deuterium-tritium fusion reaction is the most efficient fusion reaction, the radioactivity of tritium creates difficulties for experiments.[1] Molecular deuterium has properties that are similar to deuterium-tritide and is therefore used as a substitute on the basis of the high cost of tritium and safety concerns.

Extreme temperatures and pressures generally provide the energy required to initiate a fusion reaction. At these conditions the material involved is no longer gas, but rather a plasma. The plasma temperatures are over a million Kelvin and therefore the plasma cannot be directly contained using any known material. Magnetic fields must be used to contain the plasma for a reactor on earth. An example of a magnetic fusion machine, the ITER[2] Project device, is also shown in Figure 1. The ITER device is a Tokamak design, which means that it is a toroidal (doughnut shaped) fusion plasma. The plasma (not shown in Figure 1) would fill the large toroidal volume at the center of the figure. Due to its size, the ITER device is capable of generating net energy, up to 10 times the amount of energy input for short periods of time.

Cryocoolers 15, edited by S.D. Miller and R.G. Ross, Jr.

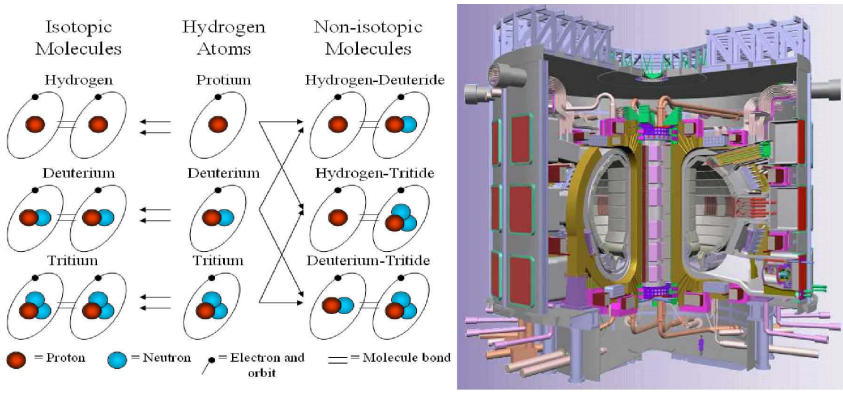

Figure 1. (Left) Protium, deuterium, and tritium atoms, isotopic molecular combinations, and non-isotopic molecular combinations. (Right) Cross-sectional rendering of the ITER device (note the person drawn for scale in the bottom of the figure) (taken from www.iter.org).

The existing design of the ITER device places constraints on the type of fuel and the method for producing and delivering the fuel. The highest temperature and densest regions of the plasma are the most likely areas for fusion to occur and these regions exist near the center of the toroidal cross-section. There are several difficulties associated with providing fuel to this region of the reactor due to the extreme temperatures, pressures, magnetic fields, and instabilities of the plasma. Although gas injectors puff fuel onto the surface of the plasma, the gas does not carry enough momentum to penetrate sufficiently far into the plasma and therefore a significant fraction of this fuel is evacuated from the reactor with the helium fusion by-product gas. In order to increase fueling efficiency, a pellet injection system supplements the puffed gas injectors.

A pellet injection system utilizes compressed gas to accelerate frozen-solid heavy hydrogen fuel pellets into the plasma. As a pellet enters the plasma, a thin layer of relatively low-temperature gas forms at its surface and protects the pellet to some extent from the plasma. It has been estimated that the pellets survive for approximately 15% of the distance into the plasma core before being completely ablated.

The specifications for the ITER device injection system are summarized below:

- 3-6 mm pellet diameter and length
- Pellet injection frequency of 7 Hz (for 6 mm pellets) to 40 Hz (for 3 mm pellets)
- Up to 500 m/s injection speed
- Continuous injection for up to 3000 seconds
- Injection volume flow rate must be equivalent to 1500 mm^3 per second
- The injection system must provide pellets to the plasma with 99% reliability.[2]

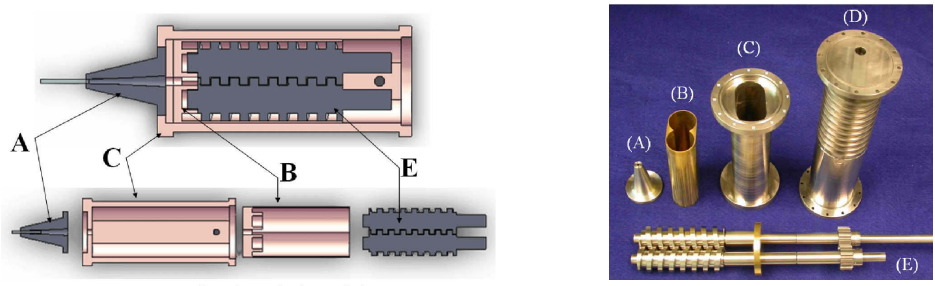

Figure 2. Cross-sectional rendering of the prototype ORNL extruder (left) and the actual extruder components prior to assembly (right): A) nozzle, B) sleeve, C) barrel, D) upper barrel, E) twin-intermeshing screws.

A continuous supply of fuel pellets is required to meet the demands of ITER. The fuel pellets are created by an extruder that solidifies fuel gas in order to create a solid rod that is subsequently cut into segments and fed to the pellet injector. Although there are a variety of extrusion strategies that can be considered, Andraschko[3] showed that twin screw extrusion is the most promising design for meeting the demands of ITER. Based on Andraschko's analysis, a prototype twin screw extruder was developed at Oak Ridge National Laboratory (ORNL) and is shown in Figure 2. The screws and upper barrel are made of 316 stainless steel, and the nozzle, sleeve, and barrel are made of oxygen free high purity copper (OFHC).

The extruder plays a dual function as it must convey and extrude hydrogen and also interface with a cryocooler in order to provide the cooling that is necessary to solidify the fuel. Deuterium solidifies at approximately 18.7 K. Although the ITER device design will have an ample supply of liquefied helium for refrigeration, the prototype extruder at ORNL operates with a Cryomech GB-37 Gifford-McMahon (G-M) cryocooler. The cryocooler is attached to the base of the copper barrel (near the nozzle) and provides cooling to the barrel.

The fueling of a fusion reactor is a demand-based process. A continuous fuel supply is required to ensure proper fuel pellet quality and quantity. The operational parameters of the extruder must be adjusted in order to meet the demanded fuel output and the design parameters must be adjusted in order to specify the optimal extruder and cryocooler operation. It is therefore desirable to have a physics-based, predictive model of the extruder that can be used to investigate extruder operation and control as well as the design and thermal management.

NUMERICAL MODEL

Extruder Geometry

The geometry associated with the intermeshing screws is complex. Ultimately, one objective of the model is to define the relationship between the rotation rate of the screws and the volume rate of material extruded. It is necessary therefore to determine the volume captured in the "C" volumes that are created between adjacent screw teeth. A model schematic of a "C" volume is shown if Figure 3. Using the parameters summarized in Table 1, White[4] provides a methodology for calculating the "C" chamber volume.

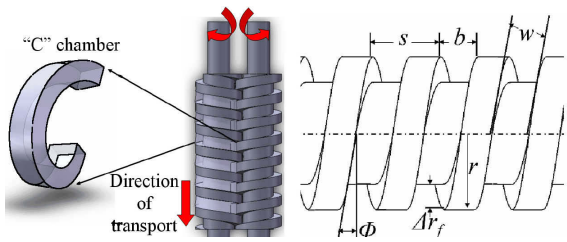

Figure 3. (Left) Model schematic of the screw intermesh region and "C" chamber. (Right) Screw geometry variables.

Table 1. Prototype ORNL screw geometry variables.

Screw geometry variable	Value
Axial distance between threads (s)	0.012 m
Axial length of thread gap (b)	0.0066 m
Thread pitch (w)	0.0065 m
Channel depth (Δr_F)	0.0045 m
Outer radius (r)	0.0135 m
Thread angle (Φ)	8.13°
Number of turns (N)	7.5
Total screw length (L)	0.09 m

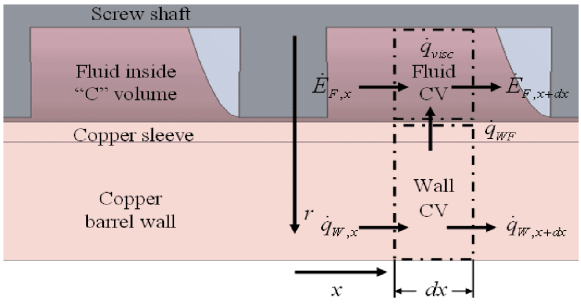

Figure 4. Control volumes describing energy transfer before solidification.

Development of the governing equations

The rate of energy transfer inside the extruder controls the solidification process and therefore the extruder operation. A set of two differential (in the axial direction) control volumes (CVs) are shown in Figure 4; the control volumes are stationary and enclose the wall material and the fluid. Figure 4 shows the heat transfer, $\dot{q}$, across the surfaces of the control volumes, the energy transported by mass flow into and out of the control volumes, $\dot{E}_F$, and the conversion of mechanical to thermal energy due to viscous dissipation, $\dot{q}_{visc}$. It is assumed that properties are isotropic in the circumferential direction. The axial position of any point on the screw does not change over time because its motion is a pure rotation. The average temperature of the material within the control volumes is time invariant at steady-state. A series of these control volumes encompasses the extruder and the control volumes are fixed with respect to the axial direction. The resistance to axial conduction through the fluid and screw shaft are approximately three orders of magnitude larger than the resistance to conduction through the copper wall; therefore, axial conduction in the fluid and screw material is neglected.

The energy balance on the wall control volume is

$$\dot{q}_{W,x} = \dot{q}_{WF} + \dot{q}_{W,x+dx} . \tag{1}$$

The axial energy transfer through the wall due to conduction is given by Fourier's law:

$$\dot{q}_{W,x} = -k_{W,x}\, A_c \frac{dT_W}{dx} , \tag{2}$$

where A_c is the cross sectional area of the extruder wall, k_W is the conductivity of the wall material, and T_W is the temperature of the wall material. The rate of heat transfer due to convection from the wall to the fluid is:

$$\dot{q}_{WF} = \bar{h}\ per\ dx \left(T_W - T_F\right) . \tag{3}$$

where *per* is the perimeter of the inner wall surface, $\bar{h}$ is the average convective heat transfer coefficient, and T_F is the mean temperature of the fluid. Substituting Eqs. (2) and (3) into Eq. (1) , expanding the $x+dx$ term and taking the limit as dx approaches zero leads to:

$$\frac{d^2 T_W}{dx^2} = \frac{\bar{h}\ per \left(T_W - T_F\right)}{k_W\ A_c} . \tag{4}$$

This equation is the governing differential equation for the wall temperature.
The steady-state energy balance on the fluid control volume is

$$\dot{E}_{F,x} + \dot{q}_{WF} + \dot{q}_{visc} = \dot{E}_{F,x+dx} . \tag{5}$$

$\dot{E}_{F,x}$ is the rate of energy transported by fluid flow

$$\dot{E}_{F,x} = \dot{m}\, i_x , \tag{6}$$

where i_x is the enthalpy of the fluid and $\dot{m}$ is the mass flow rate of the fluid. The pressure driven enthalpy change is small and therefore the change in enthalpy can be expressed as the product of the specific heat capacity at constant pressure (c_F) and the temperature gradient in the

fluid. The heat transfer into the control volume is given by Eq. (3). The generation of thermal energy within the control volume can be expressed as[5]:

$$\dot{q}_{visc} = \mu\, A_{cf}\, dx \left(\frac{per\ \omega}{\Delta r_F} \right)^2 \tag{7}$$

where μ_F is the fluid viscosity, A_{cF} is the cross sectional area of the fluid control volume, ω is the screw rotation rate, and Δr_F is the change in radius across the fluid control volume.

Equations (7) and (3) can be substituted into Eq. (5) and simplified in order to obtain the governing differential equation for the fluid temperature

$$\frac{dT_F}{dx} = \frac{\bar{h}\ per}{\dot{m}\, c_F} \left(T_W - T_F \right) + \frac{\mu\, A_{cf}}{\dot{m}\, c_F} \left(\frac{per\ \omega}{\Delta r_f} \right)^2 . \tag{8}$$

Modeling the Latent Heat of Fusion

In order to include the latent heat of solidification in the analysis, the heat capacity of the fluid experiencing phase change is artificially increased so that the enthalpy change is included. The specific heat capacity of the liquid is assumed constant at 3625 J/kg-K and the specific heat capacity of the solid is 2250 J/kg-K. The latent heat of fusion for deuterium is 4.93×10^4 J/kg. The phase change is assumed to occur over a small range of temperature rather than precisely at the solidification temperature. The range of temperatures is defined by a half-width of ΔT. When the mean temperature of the fluid is within ΔT of the triple point (T_{tp}), the effective heat capacity is taken to be the sum of the average of the liquid and solid heat capacities plus the ratio of the latent heat of fusion to the temperature range assigned to the solidification process:

$$c_{effective} = \frac{\Delta i_{fus}}{2\Delta T} + \frac{c_{liquid} + c_{solid}}{2} . \tag{9}$$

Estimating the Heat Transfer Coefficients

There are three distinct regimes within the extruder, shown qualitatively in Figure 5. Regime 1 is completely liquid that is being cooled to the triple point. Regime 2 contains a scraped surface that is partially ice fouled and includes a two-phase liquid and solid-particle mixture. Regime 3 is a sub-cooled solid. The complex geometry and dynamics of the extruder teeth make it difficult to predict the flow field exactly, even in the single phase liquid region. However, due to the extremely slow rotation speeds (5-15 rpm), the axial flow in the "C" volume has a Reynolds number of 73 corresponding to a laminar flow regime. The mixing action promoted by the screw threads will tend to enhance convection. This analysis assumes a Nusselt number of 10 using a characteristic length for heat transfer (L_{char}) that is half the distance between the screw shaft and wall (Δr_F /2) to estimate the heat transfer coefficient:

$$\bar{h}_{liquid} = \frac{Nus\ k_F}{L_{char}} , \tag{10}$$

where k_F is the conductivity of the fluid. The average convection coefficient for the liquid at a rotation rate of 7.3 rpm is 460 (W/m²-K).

The convection coefficient for the two-phase mixture is estimated as the linear combination of the solid and liquid convection coefficients

$$\bar{h}_2 = \delta_{ls}\ \bar{h}_{liquid} + \left(1 - \delta_{ls}\right) \bar{h}_{solid} . \tag{11}$$

where δ_{ls} is the fraction of the fluid that is liquid and $\bar{h}_{liquid}$ and $\bar{h}_{solid}$ are the heat transfer coefficients assuming single phase liquid and single phase solid. Eventually, the fluid has completely solidified and the extruder enters Regime 3. The convection coefficient for Regime 3 is estimated

$$\bar{h}_{solid} = \frac{k_s}{L_{cond}} , \tag{12}$$

where k_s is the thermal conductivity of the solid, and L_{cond} is the average length of heat conduction which is taken to be one half the distance between the screw shaft and wall (Δr_F /2). In the two-phase regime, the average length of solid conduction must clearly be reduced to account for the initially thin layer of ice. During the two-phase solidification region the average ice thickness and L_{cond} for the solid are nominally assumed to be 0.001 m. This reduction in the characteristic length creates an increase in the convection coefficient during Regime 2.

Modeling the energy dissipation caused by viscous shearing of solid

Equation (7) was used previously to calculate the energy generation in the fluid control volume through viscous dissipation. Meitner[5] provides some of the first experimental measurements of the effective viscosity associated with shearing solid deuterium. The measured values of the viscosity at the triple point temperature were curve fit to a function of temperature and rotation rate. The decrease in viscosity of the solid with temperature is assumed to be constant.

$$\frac{d\mu}{dT} = -\frac{4x10^4}{11}\left[\frac{Pa-s}{K}\right]. \tag{13}$$

The y-intercept of the viscosity is assumed to vary with the rotation rate. A correlation for the viscosity of shearing deuterium is therefore

$$\mu = \frac{d\mu}{dT}\left(T_F - T_{tp}\right) + \mu_0 = -\frac{4x10^4}{11}\left(T_F - T_{tp}\right) + 64.472\,\omega^{-1.5823}. \tag{14}$$

Figure 6 shows the effective viscosity predicted by Eq. (14) at various rotation speeds.

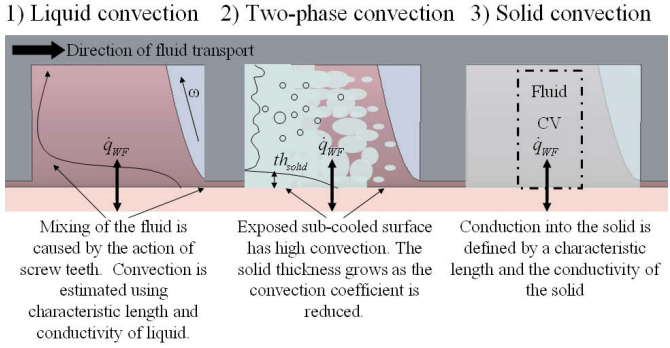

Figure 5. Three distinct phase regimes within the extruder.

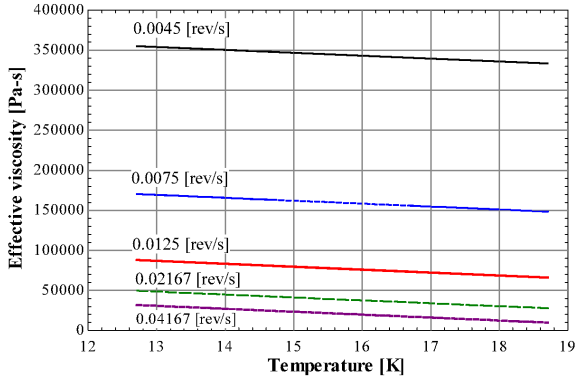

Figure 6. Effective viscosity versus temperature at various rotation rates.

Numerical Integration Technique

The governing differential equations are numerically integrated from $x = 0$ (the inlet to the extruder) to $x = L$ (the outlet of the extruder) using Euler's method implemented with uniform length steps. The maximum length step that can be tolerated before a solution becomes unstable is called the critical length step. For the numerical model of the extruder, the governing differential equation for the fluid, Eq. (8), can be investigated in order to determine the critical length step:

$$\Delta x_{crit} = \frac{\dot{m}\, c_F}{\bar{h}\ per}\,. \tag{15}$$

The critical length step occurs at the onset of solidification. For the nominal operating conditions, the critical length step is equal to 0.0115 m which is not too small relative to the axial length of the extruder. Therefore, the Euler model is adequate for this analysis. To numerically integrate the conservation equation for the extruder, Eq. (4) and Eq. (8), are written for each length step

$$\left.\frac{d^2T_W}{dx^2}\right|_{i-1} = \bar{h}_{i-1}\ per\ \frac{T_{W,i-1} - T_{F,i-1}}{\left(k_{i-1}\ A_{c,cross}\right)} \quad \text{for } i = 1...N\,, \tag{16}$$

$$\left.\frac{dT_F}{dx}\right|_{i-1} = \frac{\bar{h}_{i-1}\ per\left(T_{W,i-1} - T_{F,i-1}\right) + q_{visc,i-1}}{\left(\dot{m}\, c_{F,i-1}\right)} \quad \text{for } i = 1...N\,, \tag{17}$$

where the subscript i denotes the node number being considered and N denotes the total number of nodes. An Euler step similarly is used to predict the fluid and the wall temperature change experienced during each length step:

$$T_{F,i} = T_{F,i-1} + \left.\frac{dT_F}{dx}\right|_{i-1} \Delta x \quad \text{for } i = 1...N\,, \tag{18}$$

$$T_{W,i} = T_{W,i-1} + \left.\frac{dT_W}{dx}\right|_{i-1} \Delta x \quad \text{for } i = 1...N\,, \tag{19}$$

where Δx is the size of the length step. Because the differential equation for the wall temperature volume, Eq. (16) is second order, an additional Euler step must be included to predict the change in the wall temperature gradient over each length step:

$$\left.\frac{dT_W}{dx}\right|_{i} = \left.\frac{dT_W}{dx}\right|_{i-1} + \left.\frac{d^2T_W}{dx^2}\right|_{i-1} \Delta x \quad \text{for } i = 1...N\,. \tag{20}$$

Three boundary conditions are required by the coupled 1st and 2nd order differential equations, Eqs. (8) and (4). The physical boundary conditions associated with the problem include the inlet fluid temperature, $T_{F,1}$, which is assumed to be the normal boiling point temperature of deuterium. The extruder section that bolts to the stainless steel upper barrel is assumed to be adiabatic; therefore, the wall temperature gradient at node 1, $dT_W dx_1$, must be zero. The cryocooler is attached near the nozzle of the extruder. Therefore, the relationship between the wall temperature at node N, $T_{W,N}$, and the energy leaving node N by conduction is related to the load curve of the cryocooler. The cryocooler load curve is expressed using the empirical function[6]:

$$\dot{q}_{Cooler} = \exp\left(\frac{a + c\,T + e\,T^2}{1 + b\,T + d\,T^2 + f\,T^3}\right)(Watts) \tag{21}$$

where the parameters in Eq. (21) are a =1.5033419 (-), b = -0.22816705 (K^{-1}), c = -0.37274643 (K^{-1}), d = 0.015290951 (K^{-2}), e = 0.022506189 (K^{-2}), and f = -0.00020946823 (K^{-3}). The correlation provided by Eq. (21) is valid from 8 K to 30 K.

The Euler technique is an explicit technique that integrates from node 1 to node N. Only two of the three required boundary conditions ($T_{F,1}$ and $dT_W dx_1$) are known at node 1. The remaining boundary condition is specified at node N. Therefore, the temperature of the wall at the inlet ($T_{W,1}$) is assumed, the integration carried out, and the mismatch between the conditions at node N and the remaining boundary condition is evaluated. The model is implemented in the

Engineering Equation Solver software[7] and the native optimization algorithms are used to adjust the temperature of the wall at the inlet, $T_{W,1}$, until the axial heat transfer at the end of the extruder is equal to the cryocooler power at the corresponding temperature, $T_{W,N}$. Finally, if a target outlet fluid temperature (T_{target}) is required then the mass flow rate (which is directly proportional to the rate of rotation of the screw) is also adjusted until the fluid temperature leaving the extruder is equal to the target temperature.

RESULTS AND SENSITIVITY ANALYSIS

The model was used to predict the fluid and wall temperature distributions at rotation rates of 3.67 rpm, 7.03 rpm, 11.01 rpm, and 14.68 rpm, corresponding to volumetric flow rates of $2\text{x}10^{-7}$ m^3/s, $3.98\text{x}10^{-7}$ m^3/s, $6\text{x}10^{-7}$ m^3/s, and $8\text{x}10^{-7}$ m^3/s. The result is shown in Figure 7. The model predicts that a maximum rotation rate of approximately 14.68 rpm ensures complete solidification of the fuel. The liquid, two-phase, and solid regimes of the extruder are evident in Figure 7. The two-phase region is characterized by a very small fluid temperature gradient due to the phase change process. The transition from the two-phase to the solid regime exhibits a sharp temperature gradient due to the relatively small heat capacity of solid deuterium.

The analysis described here is based on fairly simple models of the heat transfer coefficient, viscous dissipation, and the best estimates of the thermophysical properties of the deuterium and extruder. Future research will be directed at refining the model by improving our understanding of these aspects of the extrusion process. This research is guided by a sensitivity analysis carried out using the numerical model. Nine parameters are considered in this sensitivity analysis: liquid heat capacity, solid heat capacity, the latent heat of fusion, the viscous dissipation, the solid convection coefficient, the liquid convection coefficient, the two-phase convection coefficient, and the *RRR* value (analogous to purity) of the copper barrel wall. The sensitivity of the extruder performance to each of these variables is defined by predicting the mass flow rate of fuel that can be provided by the extruder while achieving a target exit fluid temperature that ensures complete solidification with a small amount of sub-cooling. Then, each of these parameters is perturbed and the resulting change in the mass flow rate provided by the extruder is normalized by the change in the parameter. A variable with a sensitivity of 1 has, approximately, a proportionally equivalent effect on the extruder flow rate, i.e., a 10 % change in the variable changes the flow rate by 10 %. The normalized sensitivities of the parameters are shown in Figure 8.

Figure 8 indicates that the extruder performance is most sensitive to the two-phase convection coefficient, followed in order by latent heat of fusion, liquid convection coefficient, viscous dissipation, Copper purity, solid heat capacity, solid convection coefficient, and liquid heat capacity. These results suggest the most productive avenues for future research into the extrusion process.

CONCLUSIONS

A numerical model of the solidification of deuterium inside a twin screw extruder is presented. A sensitivity analysis of the flow parameters indicates that the two-phase convection coefficient is the most sensitive parameter to the model followed by the latent heat of solidification, liquid convection coefficient, and viscous dissipation. Future research efforts will focus on experimental measurements of the two-phase and liquid convection coefficients.

ACKNOWLEDGMENT

The authors acknowledge the support of the Plasma Fueling Group at Oak Ridge National Lab. This work is funded by Department of Energy grant number ER54821.

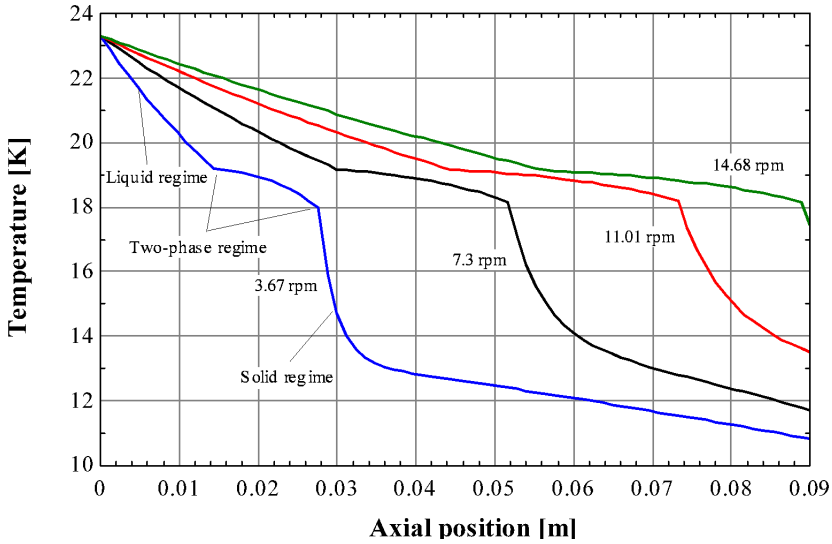

Figure 7. Axial temperature distribution of the wall and fluid predicted by the numerical model at various operation speeds.

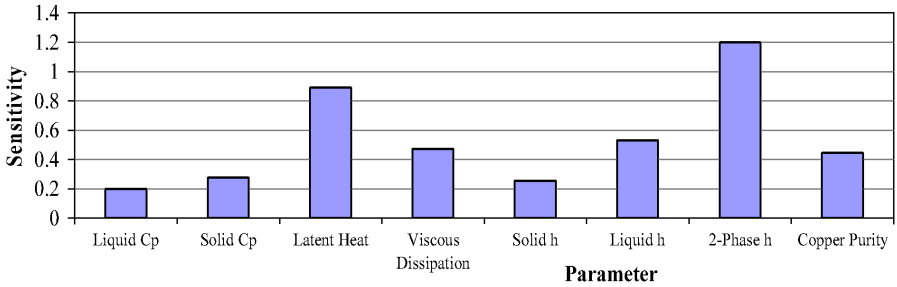

Figure 8. Sensitivity of the extrusion performance to several parameters.

REFERENCES

1. McNally, J.R., Jr., Rothe, K.E., Sharp, R.D., *Fusion Reactivity Graphs and tables for Charge Particle Reactions*, ORNL/TM-6914, Oak Ridge National Laboratory, Oak Ridge, TN (1979).
2. Spears, B., ITER, Accessed as a web page at www.iter.org.
3. Andraschko, M.R., "Twin screw extrusion and viscous dissipation for the pellet fueling of fusion reactors," Master's Thesis, University of Wisconsin-Madison (2006).
4. White, J.L., and Potente, H., "Screw Extrusion" Hanser Publishers, Munich (2002).
5. Meitner, S.J., "Viscous energy dissipation in frozen cryogens," Master's Thesis, University of Wisconsin-Madison (2008).
6. Cryomech, Inc., "Cryorefrigerator Specifications" (2001).
7. Klein, S.A., EES-*Engineering Equation Solver*, F-chart Software (2008).